

JOURNAL OF MECHANICS OF CONTINUA AND MATHEMATICAL SCIENCES

www.journalimcms.org



ISSN (Online): 2454 -7190 Vol.-20, No.-9, September (2025) pp 52 - 72 ISSN (Print) 0973-8975

SEISMIC RESISTANCE OF REINFORCED CONCRETE COLUMNS UNDER COMBINED SPECIAL ACTIONS

Ashot G. Tamrazyan¹, Tatiana A. Matsevich² Sergei Y. Savin³, Maksim V. Kudryavtsev⁴

^{1,2,3,4} Department of Reinforced Concrete & Masonry Structures, Moscow State University of Civil Engineering, Moscow, Russia.

 $Email: {}^{1}tamrazian@mail.ru, {}^{2}matseevichta@rambler.ru, {}^{3}suwin@yandex.ru \\ {}^{4}k.m.v.29.12.96@yandex.ru$

Corresponding Author: Sergei Y. Savin

https://doi.org/10.26782/jmcms.2025.09.00004

(Received: June 23, 2025; Revised: August 18, 2025; Accepted: September 04, 2025)

Abstract

The study addresses the seismic resistance of reinforced concrete columns that have been damaged by the corrosion of their steel reinforcement and the concrete itself, and that have experienced the effects of high temperatures resulting from fire. Reinforced concrete framed buildings are common in earthquake-prone regions. Such structures have a lifespan of several decades. Consequently, corrosion of the concrete and steel reinforcement is commonplace throughout their service life, particularly in coastal regions. This corrosion decreases the structures' load-bearing capacity and seismic resistance. High temperatures resulting from fires are something that such reinforced concrete framed structures are often exposed to. This study proposes and experimentally validates a design model for evaluating the load-bearing capacity and seismic resistance of such columns in buildings that have been damaged by corrosion and subsequently exposed to high temperatures. It provides a basis for assessing the safety and risk of reinforced concrete framed structures subjected to combined accidental actions, such as corrosion, high temperatures from fires, and seismic impacts.

Keywords: Reinforced Concrete, Column, Seismic Resistance, Combined Special Actions, Corrosion, Fires.

I. Introduction

Reinforced concrete framed buildings are common in earthquake-prone regions. Such structures have a lifespan of several decades. Concrete and steel reinforcement may experience corrosion during this time, particularly in coastal areas. The corrosion decreases the load-bearing capacity and seismic resistance of these structures [VII], [XII], [XVI]. A well-known example of a collapse due to corrosion damage accumulation in a reinforced concrete structure is the collapse of a condominium in Surfside, Florida, in 2021 [X].

Steel corrosion reduces the cross-sectional area of rebar, decreasing its strength and ductility. This process is accompanied by concrete cracking, which occurs due to an increase in the volume of corrosion products. This results in a weaker bond between the reinforcement and the concrete. All of these factors lead to a reduction in the structure's load-bearing capacity.

Yoon et al. [XXXIII] found that a 10-15% loss of reinforcement mass reduces the load-carrying capacity of columns by 20-30%. The development of a methodology for the evaluation of the fire resistance of reinforced concrete columns in real fire scenarios was undertaken by Kodur and Dwaikat [IX]. Chen et al. [XXXII] conducted an experimental investigation of the post-fire cyclic behavior of columns and observed a 40% reduction in energy capacity. Smolyago et al. [XX] analyzed the survey results of reinforced concrete structures with corrosion damage. This allowed them to identify the main types of structures affected by corrosion. They also examined the influence of manufacturing defects on the propagation of corrosion damage in reinforced concrete structures. The influence of concrete cover thickness on the corrosion of steel reinforcing bars was analyzed in accordance with construction standards. In [XXX], the processes of reinforcement and concrete corrosion under the influence of an aggressive medium are considered. The relationship between crack opening width and corrosion damage to reinforcing bars was revealed.

High temperatures resulting from fires are something structures made of reinforced concrete are often exposed to, as can be seen from studies [III], [XXVI], [XXVII]. High temperatures cause a loss of concrete strength; at 500-600°C, the loss is up to 50% of the initial strength. The reinforcement also becomes de-hardened, which is particularly noticeable at temperatures above 400°C. Thermal deformation can result in cracking and disruption of the bond between the rebar and the concrete. Although design standards include methods for calculating fire resistance, subsequent seismic loading is not considered.

Reinforced concrete columns are key structural elements of buildings. Damage to the columns due to corrosion or fire significantly reduces the seismic performance of facilities. The combined effects of corrosion and high temperatures accelerate structural degradation. However, this aspect is insufficiently studied. The behavior of reinforced concrete structures under combined special actions — such as aggressive environments leading to corrosion of the reinforcement and concrete, high temperatures in fires, and seismic loads — fundamentally differs from their behavior under these factors separately. This difference is due to nonlinear interaction processes in concrete and reinforcement, including degradation of mechanical properties, changes in kinematic deformation characteristics, and reduction of the structure's energy capacity. Li et al. [XIII] conducted experiments with pre-corroded specimens and observed a synergistic effect. Tamrazyan and Bariak [XXVIII] demonstrated that at high temperatures and levels of corrosion, the bonding of reinforcement to concrete decreases significantly. They provided models and analytical relationships that allow one to perform a preliminary assessment of the reliability of reinforced concrete structures and their fire resistance in the event of corrosion. Another study [VI] exposed reinforced concrete columns to corrosion until they reached a target mass loss of 30%.

Subsequent tests revealed a 40-44% reduction in the fire resistance of corrosion-damaged columns, accompanied by spalling of the concrete cover.

Investigating the residual bearing capacity and seismic resistance of columns damaged by combined special actions (CSA) is important for assessing risk and developing methods to strengthen such structures. This study aims to develop and experimentally validate design models and criteria for checking the seismic resistance of reinforced concrete columns in framed RC structures that are subject to combined special actions, such as seismic loads, corrosion damage, and high temperatures resulting from fire.

II. Models and Methods

II.i. Corrosion Behavior of Concrete and Steel Rebars

To describe the changes in strength and deformation modulus throughout the corrosion-damaged concrete layer, the degradation function [VIII], [XIX] presented in Figure 1, which was established empirically, is used. The parameters of this function depend on the type of corrosive medium and can be approximated as follows:

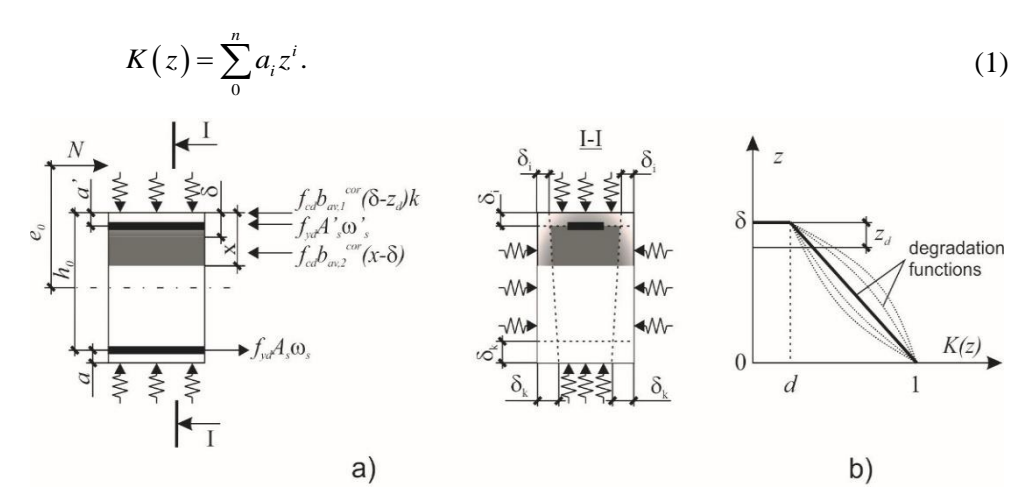


Fig. 1. Scheme for calculating an eccentrically compressed, corrosion-damaged reinforced concrete member: design section (a); general view of degradation functions of the corrosion-damaged layer (b)

The depth of corrosion damage in concrete is estimated according to the relation proposed by Popesko and considered in the study [XVII]:

$$\delta(\tau) = K\tau^m,\tag{2}$$

Where τ is the time of aggressive medium action;

K and m are the factors of aggressiveness of a particular medium to a certain type of concrete.

Based on experimental data [XVII], the following relations are obtained for the depth of corrosion damage at a given moment in time for steel reinforcing bars:

$$\delta(\tau) = \delta_k(\tau) + \Delta\delta(\tau),\tag{3}$$

where $\delta_k(\tau)$ is the depth of corrosion damage, and $\Delta\delta(\tau)$ is the increase in the rebar diameter due to corrosion products. The following relation can be used for δ_k :

$$\delta_k(\tau) = \delta_0 \left(1 - e^{-a_p \tau} \right),\tag{4}$$

where δ_0 is the initial diameter of the rebar, and a_p is the empirical factor.

II.ii. Constitutive Models of Steel and Concrete at High-Temperature Exposure

The degradation in the strength, ductility, and initial modulus of elasticity of concrete exposed to high temperatures is accounted for by partial factors γ_{bt} , ν_t , β_{bt} [XV]. These factors depend on temperature, as shown in Figure 2.

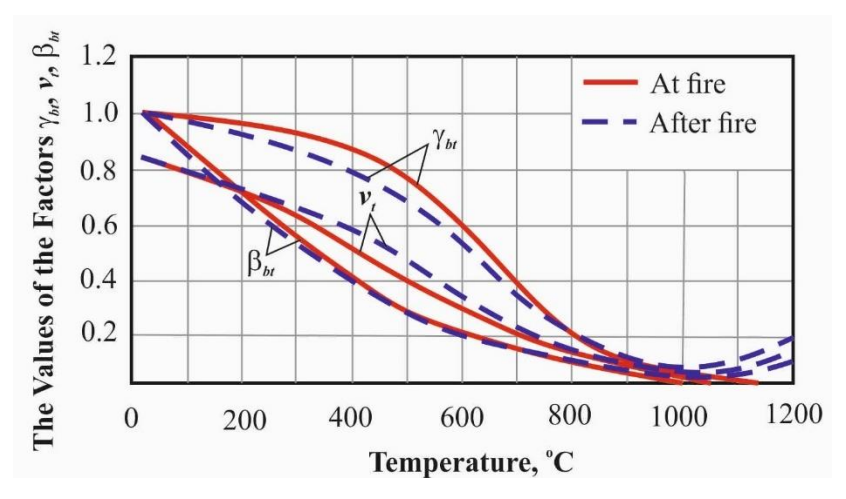


Fig. 2. The values of the factors γ_{bi} , ν_i , and β_{bi} for heavy concrete on granite aggregate during and after the fire

According to [XXVII], the decrease in the elastic modulus (E_s) values at elevated temperatures can be approximated as follows:

$$\frac{E(T)}{E} = 1 + \frac{1}{2000 \ln \frac{(T - 273)}{1100}}.$$
 (5)

The yield strength (f_{yd}) of steel rebar at heating with regard to data [V] is approximated by the relations:

$$\begin{cases} \gamma_E = 1 - 0.00033 (T - 273) & for \quad T < 773 \text{K}; \\ \gamma_E = 0.84 - 0.0012 (T - 273) & for \quad 773 \text{K} \le T < 973 \text{K}. \end{cases}$$
 (6)

Thus, if the temperature varies over time according to the diagrams in Figure 3(a), the diagram of concrete deformation in compression under high-temperature conditions can be described using three linear curves, as shown in Figure 3(b).

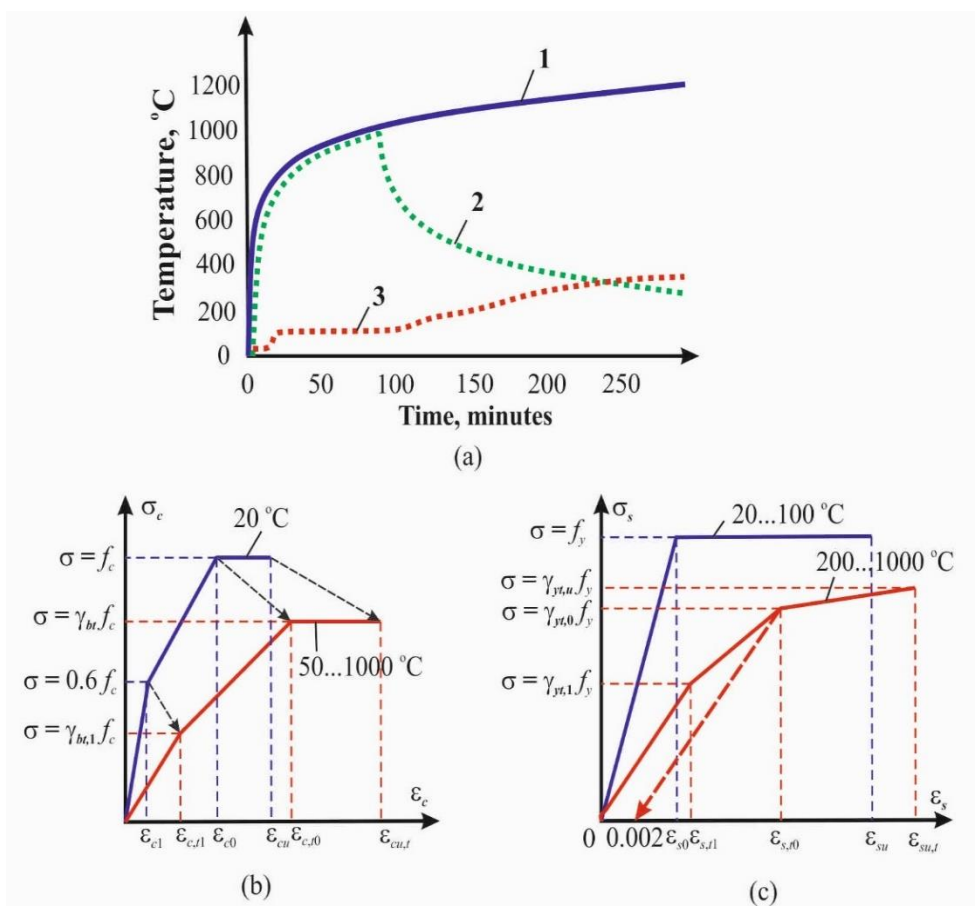


Fig. 3. Determination of concrete deformation parameters under high-temperature influence: temperature change over time (a); diagram of concrete deformation in compression under high-temperature heating (b); diagram of steel deformation with physical yield point under high-temperature heating (c). 1 - standard temperature curve according to GOST 30247-94; 2 - true temperature curve; 3 - temperature of the concrete core

II.iii. Reduction of Material Strength Under Low-Cycle Loading

Concrete subjected to low-cycle loading at high stress levels experiences a decrease in strength. According to the results of the study [XI], the strength under cyclic loading can be estimated as follows:

$$f_{c,cyc} = \gamma_{c,cyc} f_c;$$

$$\gamma_{c,cyc} = \left[\left(1.504 \eta_{top}^{0.5} - 0.11 \eta_{top}^{1.5} - 1.051 \eta_{top}^{2.5} \right) - 0.3 \ln \eta_{top} \right] \left(1 - \frac{\log N_{ult}}{2.6} \right), \tag{7}$$

where $\eta_{top} = \sigma_{c, max}/f_c$ is an upper stress level in the prism during loading.

The initial modulus of elasticity of concrete under cyclic loading:

$$E_{c,cyc} = \gamma_{E,cyc} E_c;$$

$$\gamma_{E,cyc} = \left[\left(1.816 \eta_{top}^{0.5} + 0.375 \eta_{top}^{1.5} - 1.374 \eta_{top}^{2.5} \right) - 0.3 \ln \eta_{top} \right] \left(1 - \frac{\log N_{ult}}{k_E} \right), \tag{8}$$

where k_E depends on the stress level (η^{ν}_{crc}) at the appearance of microcracks, as follows:

$$\begin{cases} k_E = 40.105 - 35.055 \frac{\eta_{top}}{\eta_{crc}^{\nu}} & \text{for} \quad \eta_{top} \le \eta_{crc}^{\nu}; \\ k_E = 5.05 & \text{for} \quad \eta_{top} > \eta_{crc}^{\nu}. \end{cases}$$

$$(9)$$

II.iv. Bond-Slip Interaction Between Steel Rebar and Concrete Under The Combined Action of Corrosion and High Temperatures

Corrosion products increase in volume when heated, creating additional pressure on the concrete cover layer [I], [II], [IV]. During heating, the corrosion products become less dense due to expansion, exerting significant pressure on the concrete and leading to the formation and opening of cracks [XVIII].

The influence of corrosion product pressure on the bond strength between rebar and concrete at high temperatures can be explained by the following empirical relationship [XXVIII]:

$$\tau(T,C) = \tau_0 (1 - 0.02)^2 \exp(-0.0011T^{1.2}), \tag{10}$$

where T is the exposure temperature in degrees Celsius and C is the degree of corrosion damage expressed as loss by mass.

Figure 4 shows the bond strength versus temperature as a function of corrosion level.

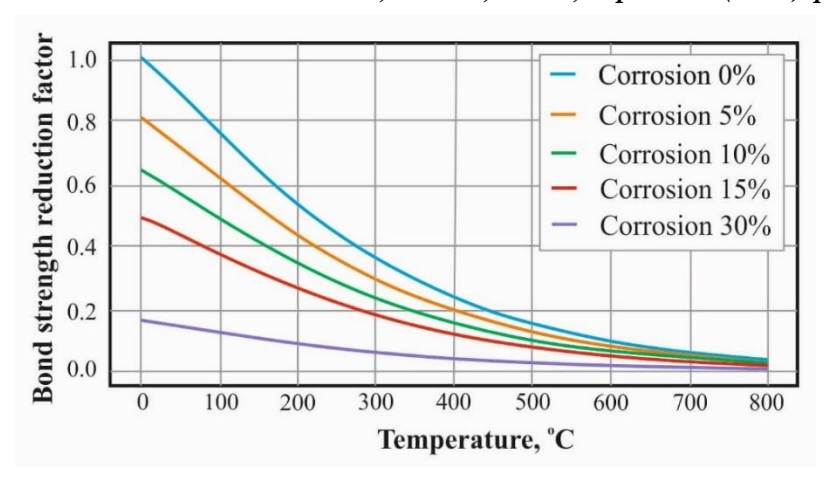


Fig. 4. The bond strength versus temperature at various corrosion levels

II.v. An Analytical Model for Seismic Resistance of Reinforced Concrete Columns Under Combined Special Actions

The seismic resistance assessment of corrosion-damaged, reinforced concrete columns in building frames, after the effects of high temperatures from fire, is based on some assumptions and limitations. This is done to obtain a suitable methodology from a design standpoint. Specifically, the columns of reinforced concrete framed structures are considered as bar elements with rigid restraints at both ends. One end is movable at the level of the upper slab, while the other end is fixed at the level of the foundation (or lower slab). The column is preloaded with a static vertical load from a special design load combination, including dead loads, long-term loads, and short-term loads, as well as a horizontal load from seismic action applied at the level of the upper floor slab, as shown in Figure 5 (a). To facilitate the analysis, the column is depicted as a cantilever bar that is half the height of a story, as illustrated in Figure 5(b).

The deformed state of the column under combined special action can be determined using a method based on nominal stiffness. As presented in this study, the nominal stiffness must account for the reduction in strength and flexural stiffness caused by corrosion damage and subsequent exposure to high temperatures. The evaluation of the column's bearing capacity and seismic resistance under combined special action is performed using hysteresis curves for the bending moment versus horizontal displacement axes. Figure 6 shows typical points of the hysteresis envelope for the column.

The analysis is based on the following assumptions regarding the deformed state of the support portions:

• The concrete's performance in the tensile zone of the support portion is ignored.

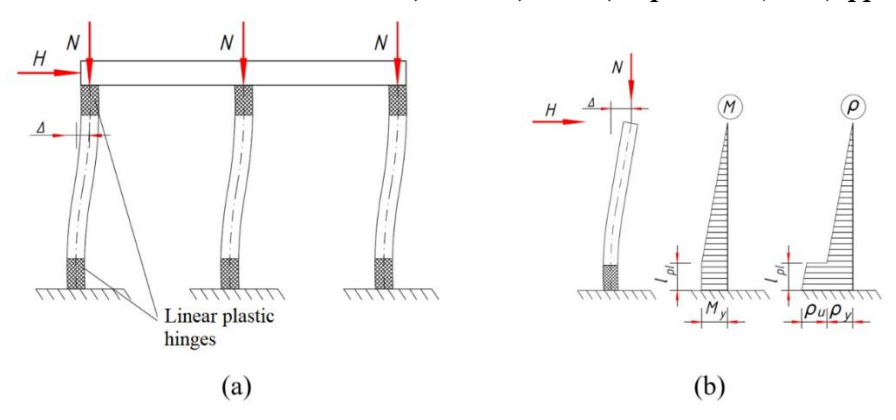


Fig. 5. Design scheme of a building frame substructure under seismic action (a); design scheme of a column (b)

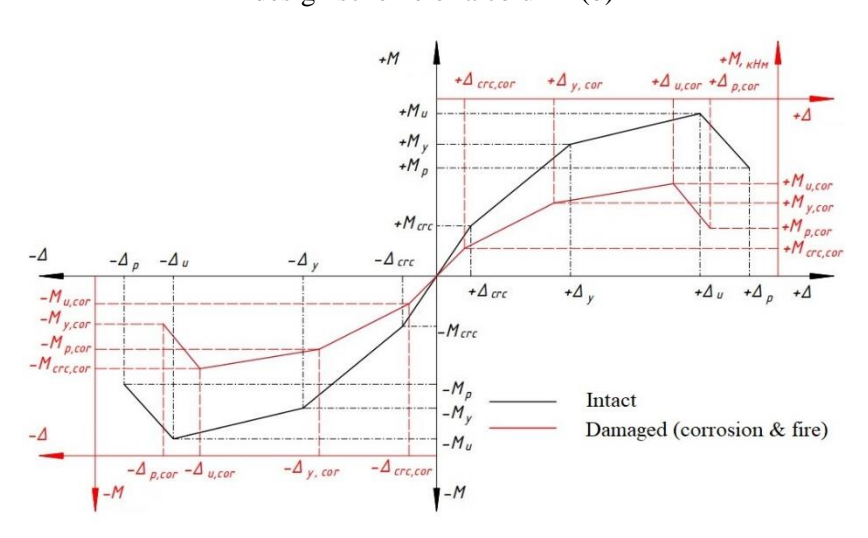


Fig. 6. Theoretical hysteresis envelope curve of the column before and after damage from corrosion and high-temperature exposure

• The strength of the concrete confined by the stirrups is adopted according to Mander et al. [XIV]:

$$f_{c,tr} = f_c + 4.1 f_e, (10)$$

where f_e is the effective lateral pressure, which for a square section column is equal to:

$$f_e = k_e \rho_s f_{sw}, \tag{11}$$

where f_{sw} is the strength of the stirrups;

 k_e is the confinement effectiveness factor that accounts for non-uniform concrete compression in cross-sections that are not circular.

 ρ_s is the volume transverse reinforcement ratio.

The strength of the cover layer's concrete is assumed to be unaffected by confinement.

The real strain diagram for the support section is bilinear due to slip between the damaged concrete and reinforcing bars caused by combined special action. Meanwhile, the design strain curve is assumed to be trapezoidal, as shown in Figure 7. This curve takes into account the reduced bonding strength of corrosion- and fire-damaged reinforcement in the concrete's compressed zone.

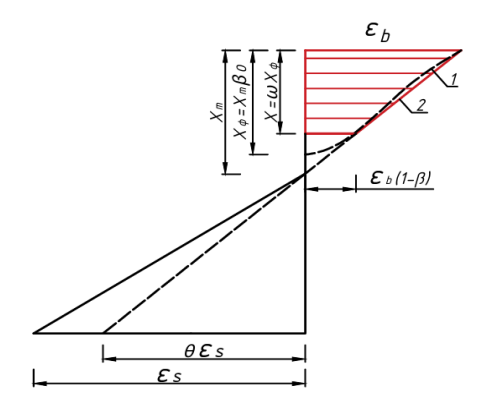


Fig.7. Strain diagram of the support section of an eccentrically compressed column: 1 – real strain curve in the concrete compression zone; 2 – design strain diagram in the concrete compression zone

The cracking moment (M_{crc}) is determined according to practice code [XXI], considering damage due to the combined effects of corrosion and subsequent high temperatures. As shown in Figure 8, areas separated by longitudinal corrosion cracks along the reinforcing bars are not accounted for in the nominal stiffness of the column.

$$M_{crc} = N\Delta_{crc} = \frac{\gamma I_{red} f_{ct}}{y_0 A_{red}} (f_{ct} A_{red} + N), \tag{12}$$

where y_0 is the distance from the tensile face to the center of gravity of the effective cross-section;

 γ accounts for the plastic behaviour of concrete, taking the value of 1.3 for a rectangular cross-section;

 A_{red} is the reduced cross-sectional area adopted for the analysis. As shown in Fig. 8(a), parts of the concrete cross-section where corrosion-related longitudinal cracks appear are excluded from the analysis:

$$A_{red} = \left(BH - 4c^2\right) + \alpha \left(A_{s,cor} + A'_{s,cor}\right),\tag{13}$$

Second-order area moment for the same cross-section:

$$I_{red} = \frac{Bb^{3}}{12} + 2\left[\frac{ec^{3}}{12} + ec\left(\frac{e+c}{2}\right)^{2}\right] + n\alpha A_{s,cor}\left(\frac{H}{2} - c\right)^{2}.$$
 (14)

The horizontal displacement of the column can be adopted as equal to the design eccentricity:

$$\Delta_{crc} = \frac{M_{crc}}{N\eta},\tag{15}$$

where η is the factor accounting for second-order effects.

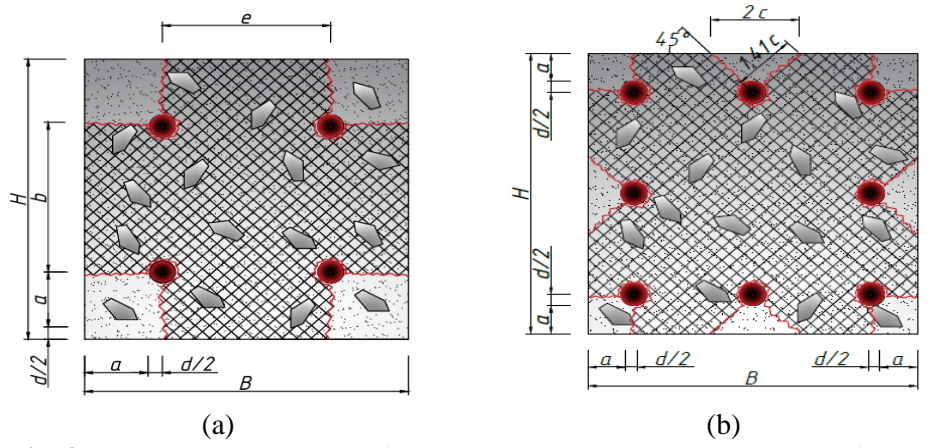


Fig. 8. Design a cross-section of the column to determine the moment of crack initiation under the action of aggressive media at all faces: rebars are arranged at the corners (a); rebars arranged on the perimeter with Z > 2C (b)

The bending moment at the beginning of the column's plastic behavior $(M_{y,csa})$ is determined as follows:

– for
$$x < c$$
:

$$M_{y} = f_{c}ex\left(h_{0} - \frac{x}{2}\right),\tag{16}$$

- for x > c:

$$M_{y} = f_{c}ec\left(h_{0} - \frac{c}{2}\right) + f_{c}\left(B - e\right)\left(x_{f} - c\right)\left(h_{0} - a' - \frac{x_{f} - c}{2}\right) + f_{c,tr}e\left(x_{f} - c\right)\left(h_{0} - a' - \frac{x_{f} - c}{2}\right) + v_{s}\varepsilon_{s}E_{s}A'_{s}\theta\left(\frac{\xi_{m} - \frac{c}{h_{0}}}{1 - \xi_{m}}\right)\left(h_{0} - c\right),$$
(17)

where θ is a factor of section deplanation. It depends on the steel reinforcement grade:

$$\theta = \frac{v_s \mu \alpha \left(1 - \xi_m\right)}{v_c \omega \beta \xi_m^2 + n_s' k_s + v_s' \mu' \alpha}.$$
(18)

To determine the deplanation factor θ , the concrete plasticity coefficients are assumed to be $v_c = 0.3$ and $\omega = 0.9$, respectively. According to the trapezoidal design strain diagram in Figure 7, $\beta(\xi_m^2)$ is the ratio of the average compressed zone depth, x_m , to the actual compressed zone depth, x.

The plasticity coefficient for reinforcement is determined using the following formula:

$$v_s = v_s' = \frac{f_y}{f_y + 400}. (19)$$

The horizontal displacement of the column corresponding to the moment $(M_{y, csa})$ is determined using formula (15).

The ultimate plastic moment ($M_{pl,csa}$) in the column support section can be defined by considering the total loss of bond between the reinforcement bars and the concrete. This can lead to a loss of stability in the compressed rebars.:

$$M_{pl} = Ne\eta = f_{c,tr} (B - 2c) x_f \left(h_0 - \frac{x_f}{2} \right) + n N_{crit,s} (h_0 - c).$$
 (20)

The moment at the ultimate horizontal displacement of the column $(M_{u,csa})$ is described by a second-order polynomial curve with variable coefficients, γ and δ , that depend on the axial force ratio of the column.

– for axial force ratio $(N/N_{ult}) = 0.3$:

$$M_{u} = (\gamma C^{2} - \delta C + 0.8) M_{pl}. \tag{21}$$

– for axial force ratio $(N/N_{ult}) = 0.6$:

$$M_{u} = (\gamma C^{2} - \delta C + 0.868) M_{pl}. \tag{22}$$

where the polynomial coefficients γ and δ are defined by linear relations:

$$\gamma = -0.0003 \left(\frac{N}{N_{ult}} \right) - 0.0003, \tag{23}$$

$$\delta = 0.0153 \left(\frac{N}{N_{ult}} \right) - 0.0086. \tag{24}$$

Linear interpolation is appropriate for determining the intermediate values of the horizontal response between the axial force ratios of 0.3 and 0.6.

III. Results and Discussion

III.i. Experimental investigations into the performance of RC columns under combined special actions

A total of 13 RC column specimens were fabricated for experimental investigation. These specimens had a square cross-section measuring 100 x 100 mm. The base of each specimen was widened to 300x300 mm and 200 mm in height to ensure rigid pinching of the column. The longitudinal load-bearing reinforcement consisted of ribbed rebar (4Ø8 A500C, μ =2.01%, As=2.01 cm²), and the concrete cover was 20 mm. The transverse reinforcement was performed using stirrups made of plain

rebars Ø6 A240; the stirrups were spaced 50 mm apart. The reinforcement scheme is shown in Fig. 9.

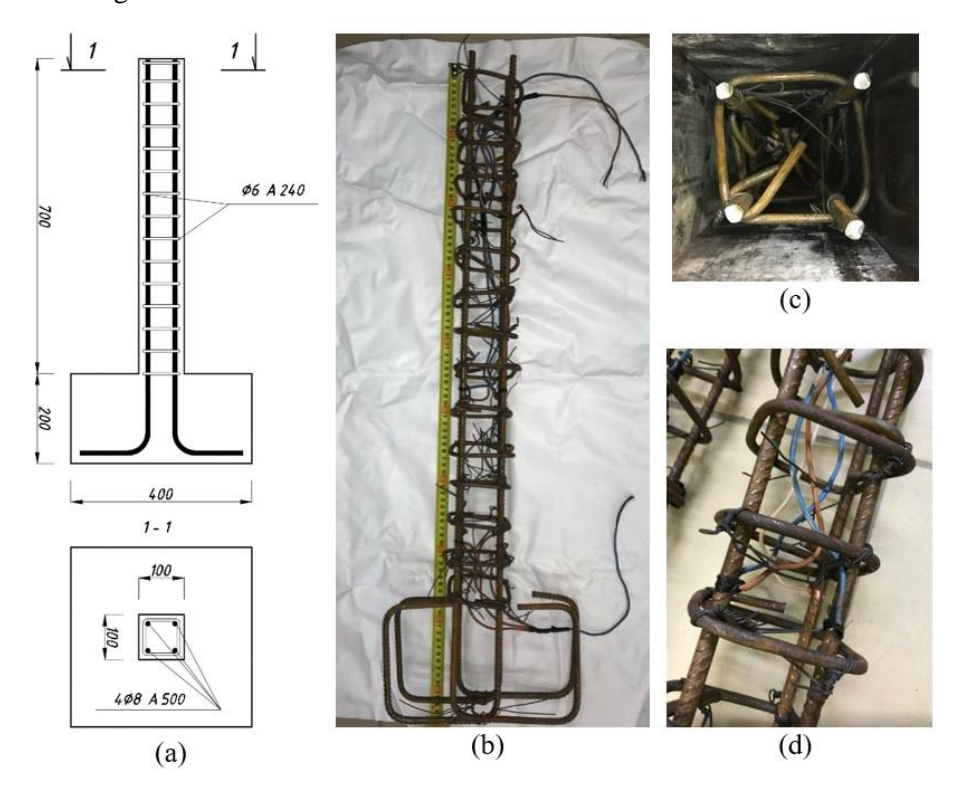


Fig. 9. Fabrication of the columns: reinforcement scheme (a); reinforcement mats assembled with copper wires (b); concrete cover control (c); fixing of copper wires to the reinforcement mats (d)

Corrosion of reinforcement in the concrete was induced by the electrochemical method by DC current action in copper conductors in the medium of 5% NaCl salt solution (Fig. 10). Wires were connected to the reinforcement mats to the power source terminal with positive charge (+). A stainless steel plate was placed in the salt solution and connected with a wire to the negative terminal (-).

All wire outputs from the reinforcement mats and stainless steel plate in the columns and in the control prisms were connected in series to the power source to the (+) terminal. The corroded specimens were placed in a large furnace for fire tests according to GOST 30247.0-94, as shown in Figure 10 (c).

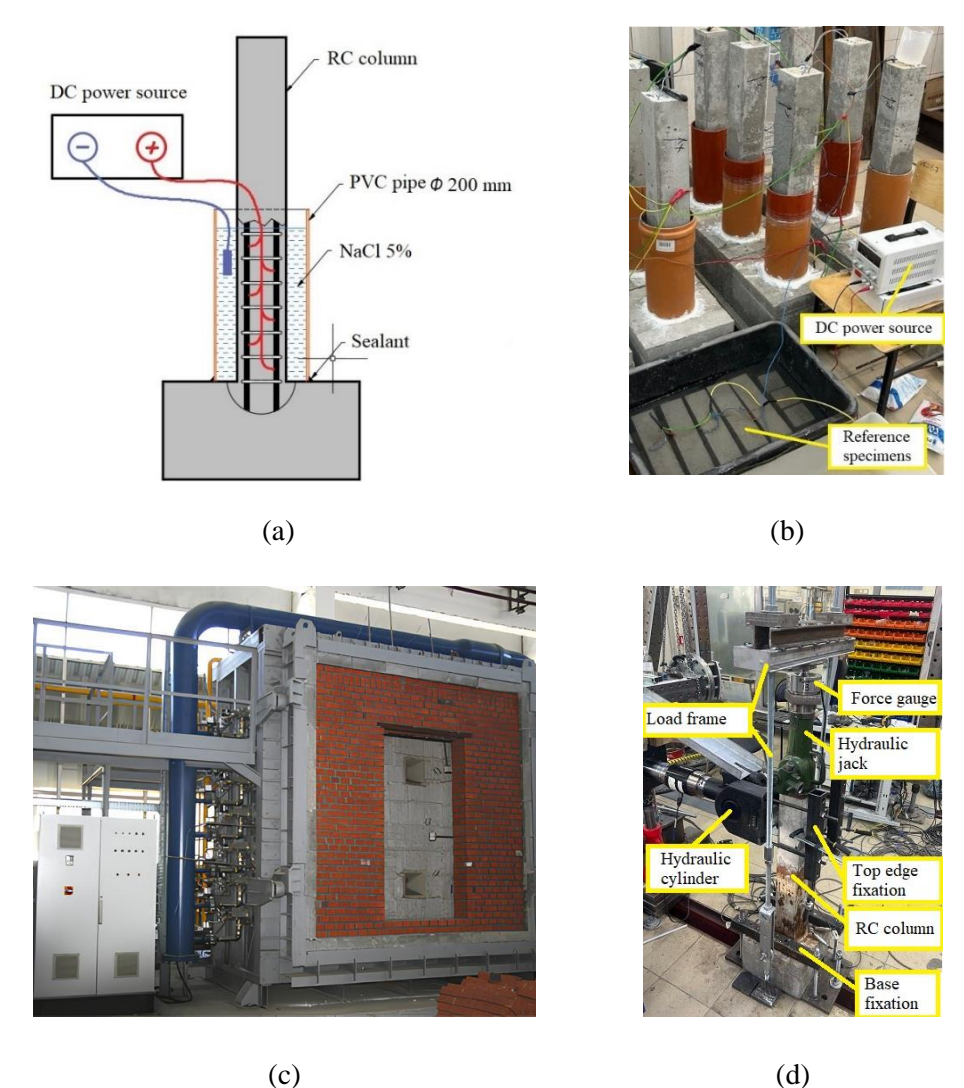


Fig. 10. Testing of specimens under combined actions: principle scheme of corrosion damage induction (a); specimens subjected to electrochemical corrosion (b); large-size furnace for testing specimens under fire conditions (c); testing of members in compression under horizontal low-cycle loadings of seismic type (d)

Corrosion of the reinforcement changes its strength and deformation characteristics. The yield and ultimate strengths of the reinforcement decreased by 6% and 11%, respectively. Significant degradation of ductility and brittle failure were also revealed.

Failure of the intact C-1.0-0 series column was observed in the lower part of the specimen at a maximum load of 250.18 kN (Fig. 11a), while failure of the corroded C-1.0-15 and C-1.0-30 series columns was detected in the damaged portion at maximum loads of 220 kN and 201 kN, respectively (Fig. 11 b, c).

The plastic failure zone in the columns of the reference series was (0.5-1)h. Stability failure of the compressed rebar was not observed in the columns. For columns with

axial force ratios of 0.3 and 0.6, the plastic failure zone was (1.0-1.5)h and (1.5-2.0)h, respectively, for columns with 15% and 30% corrosion and fire damage. Stability loss of the compressed rebars and, in some cases, rupture of the tensile reinforcement, were observed. The corrosion-related longitudinal cracks can be attributed to the increase in the plastic hinge length at the bottom portion of the column.

Table 1 shows the experimental data and their approximations using bilinear relationships. The ultimate horizontal displacement (Δ_u) is defined as the displacement that occurs when the confined concrete core is crushed or the compressed rebars lose stability. The displacement at the maximum horizontal reaction value (H_{pl}) is designated as Δ_{pl} . As shown in Table 1, the test results demonstrate a significant reduction in the load-bearing capacity of RC columns, as well as a decrease in ultimate plastic displacement under alternating loading.

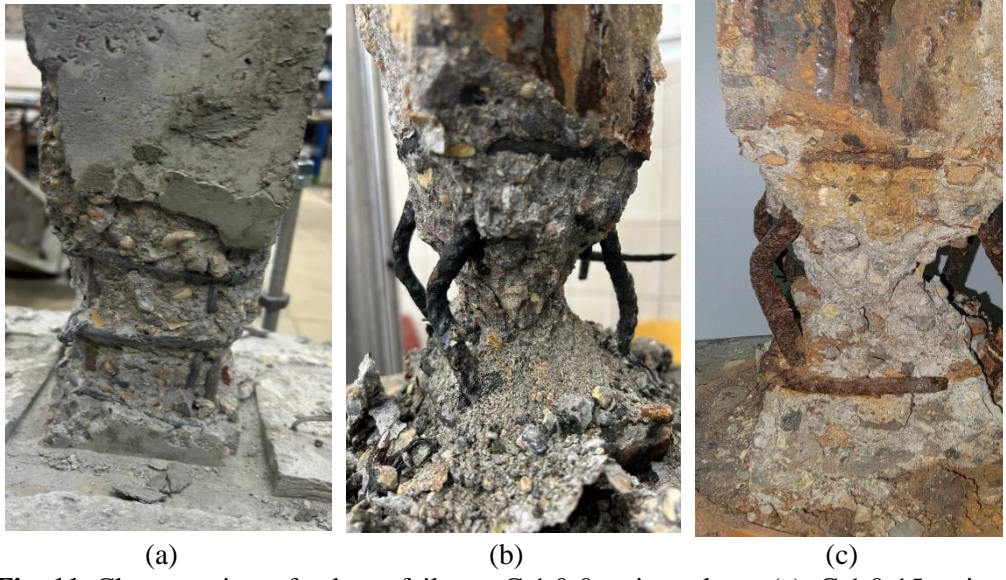


Fig. 11. Close-up view of column failures: C-1.0-0 series column (a); C-1.0-15 series columns (b); C-1.0-30 series columns (c)

Table 1: Points of the hysteresis curve envelope

No.	Specimen type	Δ_y , mm	Δ_{pl} , mm	Δ_u H_y		H_{pl}	H_u	
1	C-0.3-0	14.92	30.00	50.17	9.56	11.32	9.83	
		-15.84	-16.00	-50.21	-10.22	-10.21	-8.42	
2	C-0.7-0	10.67	24.00	40.00	8.15	9.75	8.77	
		-9.02	-20.00	-40.00	-9.53	-11.09	-8.35	
3	C-I-0.3-15	5.86	10.00	18.99	7.76	8.91	6.48	
		-6.64	-10.00	-13.99	-6.55	-7.48	-4.74	
4	C-II-0.3-15	7.19	12.03	25.02	7.32	8.56	5.81	
		-7.08	-10.01	-24.08	-7.90	-9.30	-6.79	
5	C-I-0.3-30	4.38	10.00	30.00	3.15	3.54	2.72	
		-5.96	-10.03	-33.05	-7.26	-8.54	-7.35	
6	C-II-0.3-30	6.07	10.98	29.99	5.23	6.06	3.46	
		-7.11	-12.05	-35.00	-7.54	-8.83	-8.49	

J. Mech. Cont.& Math. Sci., Vol.-20, No.- 9, September (2025) pp 52-72

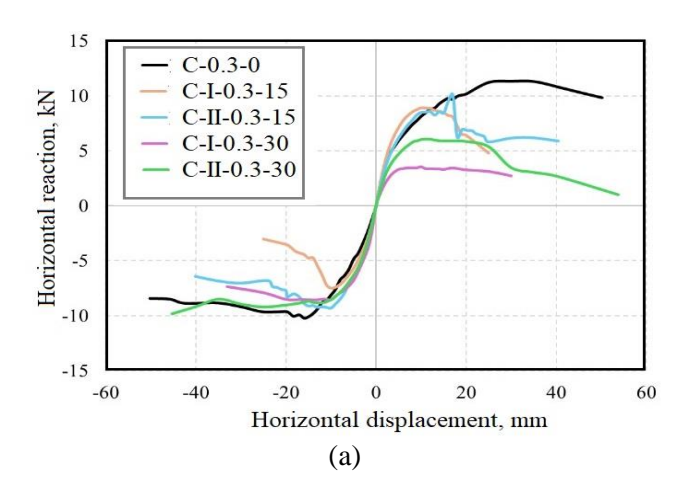
No.	Specimen type	Δ_y , mm	Δ_{pl} , mm	Δ_{u}	H_y	H_{pl}	H_u
7	C-I-0.6-15	4.38	9.99	16.99	5.02	7.25	4.09
		-5.96	-11.06	-17.00	-6.06	-8.11	-6.49
8	C-I-0.6-30	4.26	7.02	12.59	6.25	7.06	6.09
		-2.87	-4.00	-6.00	-4.17	-4.31	-3.89
9	C-II-0.6-30	6.60	10.07	16.99	5.63	6.43	4.58
		-6.53	-11.23	-18.02	-6.58	-7.33	-5.71

Note: the numerator shows values in a positive loading cycle, the denominator indicates values in a negative loading cycle.

The reduction in the load-bearing capacity of columns is associated with the combined effects of corrosion of the reinforcement and exposure to high temperatures. These effects are as follows:

- Specimens exposed to reinforcement corrosion exhibit significant cracks on the concrete surface. These cracks reduce the column's load-bearing capacity because the concrete lacks integrity and performs as separate vertical blocks.
- Reduction of the diameter of the reinforcement causes greater stress in the tensile bars at the same horizontal reaction in columns of different series. It also reduces the critical force of the compressed rebars when they lose stability.
- Reduction of the strength and ultimate strain of reinforcement due to structural damage caused by corrosion processes.
- Strength degradation of the confined concrete core within the transverse stirrups due to a reduction in the diameter of the transverse reinforcement.
- Disruption of the bonding between the rebar and the concrete leads to a decrease in the depth of the concrete compression zone and deplanation of the normal section of the column. This increases the tensile forces acting on the longitudinal rebars.

The combined special action results in a drop in horizontal reactions and amplitude displacement values. The resultant diagrams of the hysteresis curve envelopes for specimens with an axial load ratio of 0.3 and 0.6 are presented in Figure 12.



Ashot G. Tamrazian et al

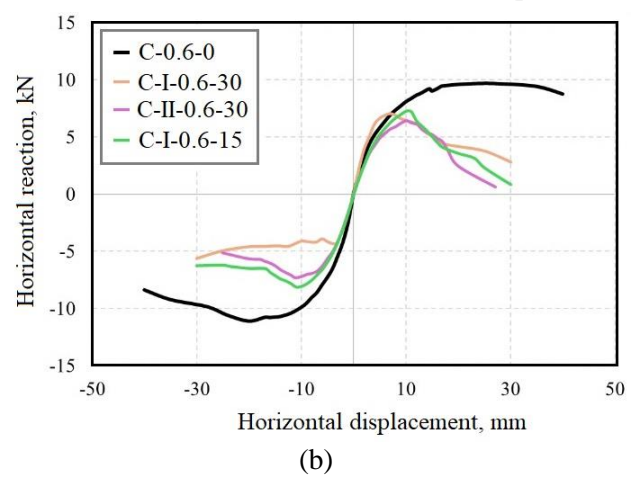


Fig. 12. Hysteresis curve envelopes: at axial force ratio of 0.3 (a); at axial force ratio of 0.6 (b)

Tests revealed a significant decrease in the first natural vibration frequency by up to 30%, as well as an increase in vibration period. Additionally, it was found that corrosion levels of 15% and 30% had almost no effect on the measured dynamic performance parameters of the columns within each series.

III.ii. Validation of the design model against experimental data

To evaluate the validity of the proposed design model, the study calculated the reinforced concrete columns tested under combined special actions. A comparison of the calculation results and experimental data is presented in Table 2 and Figure 13.

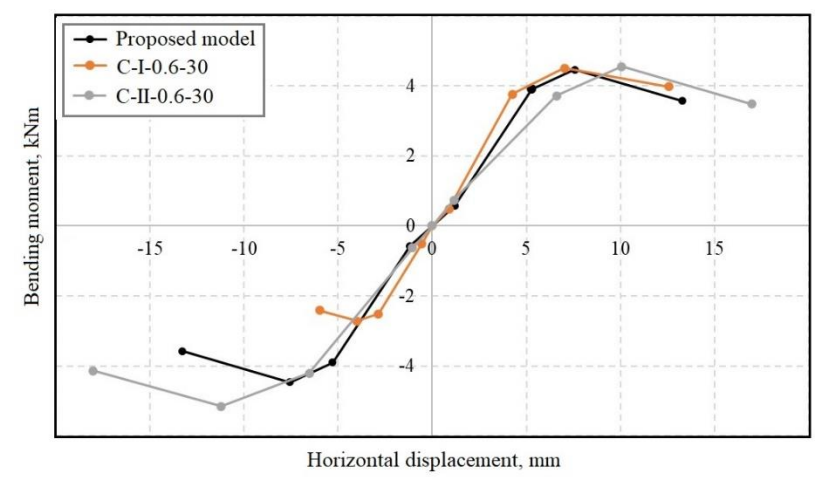


Fig. 13. Calculated and experimental hysteresis curves for reinforced concrete columns subjected to combined special actions

Table 2: Calculated and experimental hysteresis curves for reinforced concrete columns subjected to combined special actions

Proposed model								
Displacement	<i>–</i> ∆u	$-\Delta_{pl}$	– ∆y	-∆crc	∆crc	Δy	Δ_{pl}	Δu
Bending moment, kNm	-3.57	-4.47	-2.55	-0.57	0.57	2.55	4.47	3.57
Horizontal displacement, mm	-11.13	-7.57	-5.32	-1.19	1.19	5.32	7.57	11.13
Experimental specimen C–I–0.7–30								
Bending moment, kNm	-2.41	-2.72	-2.51	-0.50	0.49	3.76	4.51	3.98
Horizontal displacement, mm	-6.00	-4.00	-2.87	-0.55	1.10	4.26	7.02	12.59
Experimental specimen C–II –0.7–30								
Bending moment, kNm	-4.14	-5.16	-4.21	-0.63	0.74	3.72	4.55	3.48
Horizontal displacement, mm	-18.02	-11.23	-6.53	-1.05	1.15	6.60	10.07	16.99

A comparison of the calculation results with experimental data revealed discrepancies in bending moments of over 5% and deformations of up to 18%. This confirms the reliability of the proposed design model for reinforced concrete columns in building frames subjected to combined special actions.

The design model proposed in this paper for assessing the load-bearing capacity and seismic resistance of reinforced concrete columns in framed structures can be applied to optimize facilities, taking into account the risk of combined special actions: corrosion damage to concrete and reinforcement, as well as subsequent high-temperature exposure from fire. This problem can be solved using a genetic algorithm, the application of which to similar problems is discussed in detail in [XXII], [XXIII], [XXIV]. Following the approach considered in those studies, the solution is performed on the formed areas of permissible values of variable parameters, represented by discrete sets of values. Such parameters include strength and stiffness parameters, which can be established based on the model proposed in this study for combined special actions. Performing optimization, one of the main restrictions is the value of the cost expression of the risk of material losses in the event of a possible structural failure. In this case, a controlled random change operator [XXV] is used to search for solutions in an iterative process.

IV. Conclusions

The study considered the influence of combined special actions—comprising corrosion damage and subsequent high-temperature fire effects—on the bearing capacity and seismic resistance of reinforced concrete columns in building frames. Based on the research, the following conclusions can be drawn:

I. A design model has been proposed to assess the load-bearing capacity and seismic resistance of reinforced concrete columns in building frames that have been damaged by corrosion and the subsequent high-temperature effects of fire. This accounts for the decrease in strength and ultimate strain of concrete and reinforcement under combined action.

II. The proposed design model was validated by comparing the calculation results with data from experimental studies on the seismic resistance of reinforced concrete columns damaged by corrosion and high-temperature fires. Discrepancies in bending moments did not exceed 5%, and discrepancies in deformations did not exceed 18%. These results confirm the reliability of the proposed design model.

III. The results of the study provide a basis for assessing the safety and risk of reinforced concrete framed structures subjected to combined accidental actions, such as corrosion, high temperatures from fires, and seismic impacts. It can also be applied to solving problems of optimizing reinforced concrete framed structures, taking into account the risk of combined special actions.

V. Acknowledgements

The research was funded by the National Research Moscow State University of Civil Engineering (grant for fundamental scientific research, project No. 02-661/130).

Conflict of Interest:

There was no relevant conflict of interest regarding this article.

References

- I. Andrade C., Alonso C., : 'Test Methods for On-Site Corrosion Rate Measurement of Steel Reinforcement in Concrete by Means of the Polarization Resistance Method'. *Mater Struct*. Vol. 37, pp. 623–633, 2004.
- II. Andrade C., Cesetti A., Mancini G., Tondolo F., : 'Estimating Corrosion Attack in Reinforced Concrete by Means of Crack Opening'. *Structural Concrete*. Vol. 17, pp. 533–540, 2016. 10.1002/suco.201500114.
- III. Avetisyan L.A., Chapidze O.D., : 'Estimation of Reinforced Concrete Seismic Resistance Bearing Systems Exposed to Fire'. IOP Conf Ser Mater Sci Eng. Vol. 456, 2018. 10.1088/1757-899X/456/1/012035
- IV. Bertolini L., Elsener B., Pedeferri P., Redaelli E., Polder R.B., : 'Corrosion of Steel in Concrete: Prevention, Diagnosis, Repair'. *Wiley*, 2013
- V. Capua D.D., Mari A.R., : 'Nonlinear Analysis of Reinforced Concrete Cross-Sections Exposed to Fire'. *Fire Saf J.* Vol. 42, pp. 139–149, 2007.
- VI. Chandra S., Sharma U.K., : 'Fire Performance of Aged and Corroded Reinforced Concrete Columns'. *Journal of Building Engineering*. Vol. 95, 2025. 10.1016/j.jobe.2024.110176.

- J. Mech. Cont.& Math. Sci., Vol.-20, No.- 9, September (2025) pp 52-72
- VII. Hayati N., Hamid A., : 'Seismic Performance of Interior Beam-Column Joint With Fuse-Bar Designed Using EC8 Under In-Plane Lateral Cyclic Loading'. In Proceedings of the International Conference on Disaster Management and Civil Engineering (ICDMCE'15) Oct. 1-3, 2015 Phuket (Thailand); Universal Researchers, October 1 2015.
- VIII. Huang T., Wan C., Liu T., Miao C., : 'Degradation law of bond strength of reinforced concrete with corrosion-induced cracks and machine learning prediction model'. Journal of Building Engineering. Vol. 98, no, 111022, 2024. 10.1016/j.jobe.2024.111022
 - IX. Kodur V.K.R., Dwaikat M.M., : 'Effect of Fire Induced Spalling on the Response of Reinforced Concrete Beams'. *Int J Concr Struct Mater*. Vol. 2, pp. 71–81, 2008. 10.4334/IJCSM.2008.2.2.071.
 - X. Kong X., Smyl D., : 'Investigation of the Condominium Building Collapse in Surfside, Florida: A Video Feature Tracking Approach'. *Structures*. Vol. 43, pp. 533–545, 2022. 10.1016/j.istruc.2022.06.009.
 - XI. Kudryavtsev M.V., : 'Strength and deformability of concrete under low-cycle loading'. *Innovation and Investment*. Vol. 5, pp. 195-201, 2022.
- XII. Levtchitch V., Kvasha V., Boussalis H., Chassiakos A., Kosmatopoulos E., ; 'Seismic Performance Capacities of Old Concrete'. In Proceedings of the 13 th World Conference on Earthquake Engineering, Vancouver, B.C., Canada; 2004; pp. 1–15.
- XIII. Li X., Miao J., Zhou Y., Shi P., Wang W., : 'Experimental Study on Seismic Performance of Corroded RC Frame Joints after Fire'. *Jianzhu Jiegou Xuebao/Journal of Building Structures*. Vol. 39, pp. 84–92, 2018.
- XIV. Mander J.B., Priestley J.N., Park R.,: 'Theoretical Stress-Strain Model for Confined Concrete'. *Eng Struct*. Vol. 116, pp. 1804–1825, 1989.
- XV. Okolnikova G.E., Ershov M.E., Malafeev A.S.,: 'The effect of defects and damages in reinforced concrete load-bearing structures on further operating conditions'. *Journal of Mechanics of Continua and Mathematical Sciences*. Vol. 19, no. 7, pp. 1-16, 2024. 10.26782/jmcms.2024.07.00001
- XVI. Park R., : 'A Summary of Results of Simulated Seismic Load Tests on Reinforced Concrete Beam-Column Joints, Beams and Columns with Substandard Reinforcing Details'. *Journal of Earthquake Engineering*. Vol. 6, pp. 147-174, 2002. 10.1080/13632460209350413.
- XVII. Popov D.S., : 'Experimental studies of dynamic properties of corrosion-damaged compressed reinforced concrete elements'. *Building and reconstruction*. Vol. 100, pp. 55-64, 2022. 10.33979/2073-7416-2022-100-2-55-64

- J. Mech. Cont.& Math. Sci., Vol.-20, No.- 9, September (2025) pp 52-72
- XVIII. Saad M., Abo-El-Enein S.A., Hanna G.B., Kotkata M.F., : 'Effect of Temperature on Physical and Mechanical Properties of Concrete Containing Silica Fume'. *Cem Concr Res.* Vol. 26, pp. 669–675, 1996.
 - XIX. Savin S.Yu., Kolchunov V.I., Fedorova N.V., : 'Ductility of Eccentrically Compressed Elements of RC Frame Damaged by Corrosion under Accidental Impacts'. *Reinforced concrete structures*. Vol. 1(1), pp. 46-54, 2023. https://www.g-b-k.ru/jour/article/view/8.
 - XX. Smolyago G.A., Dronov V.I., Dronov V.A., Merkulov, S.I.,: 'Investigation of influence of defects of reinforced concrete structures on corrosion processes of steel reinforcement'. *Industrial and civil engineering*. Vol. 12, pp, 25-27, 2014.
 - XXI. SP 63.13330. Concrete and reinforced concrete structures. General provisions. SNiP 52-01-2003. Standardinform, Moscow, Russia, 2018
- XXII. Tamrazyan A., Alekseytsev A.V., : 'Optimization of reinforced concrete beams under local mechanical and corrosive damage'. *Engineering Optimization*. Vol. 55(11), pp. 1905–1922, 2022. 10.1080/0305215X.2022.2134356
- XXIII. Tamrazyan A., Alekseytsev A., : 'Assessment of mechanical safety of costoptimized reinforced concrete structures'. *IOP Conf. Ser.: Mater. Sci. Eng.* Vol. 1030, 012035. 2021, 10.1088/1757-899X/1030/1/012035
- XXIV. Tamrazyan A., Alekseytsev A., : 'The efficiency of varying parameters when optimizing reinforced concrete structures'. *E3S Web Conf.* Volume 263. 2021. 10.1051/e3sconf/202126302001
- XXV. Tamrazyan A.G., Alekseytsev A.V., : 'Evolutionary Optimization of Normally Operated Reinforced Concrete Beam Structures Taking into Account the Risk of Accidents'. *Promyshlennoe i grazhdanskoe stroitel'stvo [Industrial and Civil Engineering].* No. 9, pp. 45-50. 2019. 10.33622/0869-7019.2019.09.45-50
- XXVI. 22 Tamrazyan A.G., Matseevich T.A., : 'Estimation of Damage Degree of Buildings in Earthquakes by Statistical Modeling Method'. *Reinforced concrete structures*. Vol. 7(3), pp. 3-11, 2024. 10.22227/2949-1622.2024.3.3-11
- XXVII. 23 Tamrazyan A., Kabantsev O., Matseevich T., Chernik V., : 'Estimation of the Reduction Coefficient When Calculating the Seismic Resistance of a Reinforced Concrete Frame Building after a Fire'. *Buildings.*, Vol. 14, no. 2421. 2024. 10.3390/buildings14082421.
- XXVIII. 24 Tamrazyan A.G., Baryak D.S., : 'Bonding of Corrosion-Damaged Reinforced Concrete Elements in Case of Fire Impact'. *Building and Reconstruction*. Vol. 1, pp. 40–47, 2025. 10.33979/2073-7416-2025-117-1-40-47

- J. Mech. Cont.& Math. Sci., Vol.-20, No.- 9, September (2025) pp 52-72
- XXIX. 25 Tamrazyan A.G., Kudryavtsev M.V., : 'Effect of Reinforcement Corrosion Damage on Dynamic Behavior of Compressed Reinforced Concrete Structures'. *Building and Reconstruction*. Vol. 2, pp. 81–93, 2025. 10.33979/2073-7416-2025-118-2-81-93.
- XXX. 26 Turan A.İ., Kumbasaroglu A., Yalciner H., Ayaz Y., : 'Prediction of Seismic Performance Levels of Corroded RC Frames Based on Crack Width'. *Structures*. Vol. 76, no. 108860, 2025. 10.1016/j.istruc.2025.108860.
- XXXI. 27 Wang H., Su Y., Zeng Q., : 'Design Methods of Reinforce Concrete Frame Structure to Resist Progressive Collapse in Civil Engineering'. *Systems Engineering Procedia*. Vol. 1, pp. 48–54, 2011.
- XXXII. 28 Wen Q., Chen M., : 'Study on the Nonlinear Performance Degradation of Reinforced Concrete Beam under Chloride Ion Corrosion'. *Eng Fail Anal*, Vol. 124, 2021. 10.1016/j.engfailanal.2021.105310.
- XXXIII. 29 Yoon S., Wang K., Weiss W.J., : 'Interaction between Loading, Corrosion, and Serviceability of Reinforced Concrete'. *ACI Structural Journal*. Vol. 97(6), pp. 637-644, 2000.